

Dynamic Memory Compression: Retrofitting LLMs for Accelerated Inference

Piotr Nawrot^{*QV} Adrian Łańcucki^{*QK} Marcin Chochowski^Q David Tarjan^Q Edoardo M. Ponti^V
^QNVIDIA ^KUniversity of Wrocław ^VUniversity of Edinburgh

Abstract

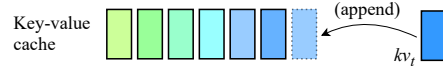
Transformers have emerged as the backbone of large language models (LLMs). However, generation remains inefficient due to the need to store in memory a cache of key–value representations for past tokens, whose size scales linearly with the input sequence length and batch size. As a solution, we propose Dynamic Memory Compression (DMC), a method for on-line key–value cache compression at inference time. Most importantly, the model learns to apply different compression rates in different heads and layers. We retrofit pre-trained LLMs such as Llama 2 (7B, 13B and 70B) into DMC Transformers, achieving up to $\sim 3.7\times$ throughput increase during auto-regressive inference on an NVIDIA H100 GPU. DMC is applied via continued pre-training on a negligible percentage of the original data without adding any extra parameters. We find that DMC preserves the original downstream performance with up to $4\times$ cache compression, outperforming up-trained grouped-query attention (GQA). GQA and DMC can be even combined to obtain compounded gains. As a result DMC fits longer contexts and larger batches within any given memory budget.

1. Introduction

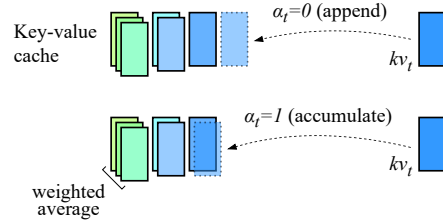
Transformer Large Language Models (LLMs) are the state of the art in generative and conversational AI (Touvron et al., 2023; Jiang et al., 2023). Their deployment, however, is curtailed in part by their inefficiency. This is not only due to the quadratic complexity of attention layers (Bahdanau et al., 2014; Vaswani et al., 2017): during generation, Transformers store the keys and values of past tokens in memory to avoid recomputing them multiple times. Since this key–value (KV) cache grows linearly with the sequence length and batch size, generation with Transformers quickly be-

^{*}Equal contribution.

Correspondence to: Piotr Nawrot <piotr.nawrot@ed.ac.uk>.



(a) Regular key–value cache with items kv_i depicted as boxes. New items are always appended.



(b) Dynamic Memory Compression (DMC) chooses whether to accumulate or append current items, resulting in a smaller key–value cache.

Figure 1: Key–value cache update mechanisms.

comes prohibitive due to the excessive memory load. This issue emerges even more clearly with long-context generation (e.g., in dialogues and stories) or when serving large numbers of user queries.

A widespread solution to increase the memory efficiency of Transformers during inference is Grouped Query Attention (GQA; Ainslie et al., 2023; Shazeer, 2019), which uses a number of key and value heads inferior to the number of query heads through parameter sharing. As an alternative, the number of overall tokens in memory can be reduced through token merging (Zhang et al., 2018; Liu et al., 2018; Bolya et al., 2022) or token pruning (Anagnostidis et al., 2023; Kim & Cho, 2020). Nevertheless, these methods often pay the price of a severe degradation in downstream performance. On the other hand, hardware/I/O-aware (Dao et al., 2022; Kwon et al., 2023) and sub-quadratic algorithms for attention (Beltagy et al., 2020; Choromanski et al., 2020) do not alleviate the memory load of the KV cache.

In our work, we aim to achieve a lossless compression of the KV cache of LLMs, thus retaining their performance while reducing their memory load. To this end, we propose Dynamic Memory Compression (DMC). As shown in Figure 1, during every time step, DMC decides whether to append

the current key and value representations to the cache or to perform a weighted average of them with the top item on the cache. Note that memory grows sub-linearly in DMC, which therefore falls halfway between vanilla Transformers and state space language models (Fu et al., 2023; Gu & Dao, 2023), where memory is constant.

In our experiments, we equip pre-existing LLMs—such as Llama 2 (Touvron et al., 2023) 7B, 13B, and 70B—with DMC by retrofitting them on a negligible percentage of the original pre-training data (~2% for 2× compression and ~4% for 4× compression) and without adding any extra parameters to the original LLM. We evaluate our DMC models on a series of downstream tasks such as MMLU (Hendrycks et al., 2021) for factuality, QA datasets for common-sense reasoning, and HumanEval (Chen et al., 2021) for code. We find that DMC LLMs retain a downstream performance similar to the original LLM, whereas GQA incurs significant degradation. Finally, we show that DMC can be hybridized with GQA such that their compression rates are compounded. For Llama 2 70B, which is pre-trained with GQA 8×, DMC 2× achieves a total compression of 16×.

We verify that KV cache compression translates into more efficient generation in practice. We measure that DMC 4× increases the inference throughput between 340% and 370% for Llama 2 7B and 13B on NVIDIA H100 or A100 GPUs without loss in performance. In fact, it allows us to fit larger batches and longer sequences into a given memory budget. Finally, compression schemata learned by DMC provide insights into the internal structure of the LLMs, revealing a preference for compressing heads in higher layers.

2. Background

2.1. Multi-Head Self-Attention

Let $X = (\mathbf{x}_1, \dots, \mathbf{x}_n) \in \mathbb{R}^{n \times d}$ denote the input sequence of hidden states of a Transformer layer, where n stands for the number of tokens in a sequence, and d for the hidden state dimension. A Multi-head Self-Attention (MHSA) layer divides the embeddings into n_h different heads. Afterwards, the self-attention process is applied to each head separately. This enables the model to focus on different parts of the input, capturing various types of relationships in the data. For each head h , different weight matrices $W_q^h, W_k^h, W_v^h \in \mathbb{R}^{d/n_h \times d/n_h}$ are used to project the input sequence into queries Q^h , keys K^h , and values V^h :

$$Q^h = (W_q^h \mathbf{x}_1, \dots, W_q^h \mathbf{x}_n) \quad (1)$$

$$K^h = (W_k^h \mathbf{x}_1, \dots, W_k^h \mathbf{x}_n) \quad (2)$$

$$V^h = (W_v^h \mathbf{x}_1, \dots, W_v^h \mathbf{x}_n). \quad (3)$$

The attention scores and outputs for the i -th token are then computed as

$$a_{ij}^h = \frac{\exp(\mathbf{q}_i^{h\top} \mathbf{k}_j^h / \sqrt{d_h})}{\sum_{t=1}^i \exp(\mathbf{q}_i^{h\top} \mathbf{k}_t^h / \sqrt{d_h})}, \quad \mathbf{o}_i^h = \sum_{j=1}^i a_{ij}^h \mathbf{v}_j^h. \quad (4)$$

Finally, the outputs from all heads are concatenated and linearly transformed to produce the final output $O \in \mathbb{R}^{n \times d}$:

$$O = (W_o[\mathbf{o}_1^1, \dots, \mathbf{o}_1^{n_h}], \dots, W_o[\mathbf{o}_n^1, \dots, \mathbf{o}_n^{n_h}]) \quad (5)$$

where $W_o \in \mathbb{R}^{d \times d}$.

2.2. KV Caching During Inference

In a Transformer decoder, the generation of sequences is auto-regressive: each new token is predicted based on the previously generated ones. To avoid redundant computation, it is common to store the keys and values of previously computed tokens in the KV cache. For each time step i , only the keys and values for the current token \mathbf{x}_i are computed whereas those for $\mathbf{x}_{<i}$ are retrieved from the cache. Thus for each head h :

$$K^h = [K_{1:i-1}^h, W_k^h \mathbf{x}_i] \quad (6)$$

$$V^h = [V_{1:i-1}^h, W_v^h \mathbf{x}_i] \quad (7)$$

Note that this process is not necessary for queries as only the query for the current token \mathbf{x}_i is needed at each inference time step.

As a consequence, the KV cache grows linearly with each new token. This progressive expansion leads to substantial memory consumption and increased latency, especially for long input sequences. This issue is further exacerbated when serving multiple requests concurrently, as each inference process requires its own KV cache, significantly straining the system’s resources.

3. Method: Dynamic Memory Compression

Inference with LLMs tends to be memory bound rather than compute bound, as we explain in Appendix A in detail. This means that latency scales linearly with the size of the KV cache. We tackle the problem of reducing the size of KV cache which brings two immediate benefits (Zhang et al., 2023): 1) it lowers the latency of auto-regressive generation, and 2) increases throughput by saving GPU memory and allowing for larger batch sizes or sequence lengths.

In this section we introduce Dynamic Memory Compression (DMC), a simple and inexpensive method for on-line compression of the KV cache at inference time. In what follows, we first describe the inference-time operation of DMC, which constitutes our end goal. Next, we illustrate how to teach a pre-trained LLM such behavior through short, continued pre-training.

3.1. Inference

Consider the forward pass of an attention layer during autoregressive inference (Section 2.1). In a vanilla Transformer, at every time step t , both \mathbf{k}_t and \mathbf{v}_t are appended to the KV cache (Section 2.2). In DMC, on the other hand, the KV cache update procedure is different, as detailed in Algorithm 1. First, a decision variable $\alpha_t \in \{0, 1\}$ and importance variable $\omega_t \in [0, 1]$ are predicted. In order to avoid adding new parameters, we reuse the first neuron from \mathbf{k}_t and \mathbf{q}_t , respectively, to extract the two scores.¹

Algorithm 1 Single-head KV cache update with Dynamic Memory Compression (DMC)

```

1: procedure KV-UPDATE( $K, V, \mathbf{q}_t, \mathbf{k}_t, \mathbf{v}_t$ )
2:    $\alpha_t \leftarrow \text{round}(\text{sigmoid}(\mathbf{k}_t[0]))$ 
3:    $\omega_t \leftarrow \text{sigmoid}(\mathbf{q}_t[0])$ 
4:   if  $\alpha_t = 1$  then ▷ ACCUMULATE
5:      $z_t \leftarrow z_{t-1} + \omega_t$ 
6:      $K \leftarrow [K_{1:l-1}, (\mathbf{k}_t z_{t-1} + \mathbf{k}_t \omega_t) / z_t]$ 
7:      $V \leftarrow [V_{1:l-1}, (\mathbf{v}_t z_{t-1} + \mathbf{v}_t \omega_t) / z_t]$ 
8:   else ▷ APPEND
9:      $z_t \leftarrow \omega_t$ 
10:     $K \leftarrow [K_{1:l}, \mathbf{k}_t]$ 
11:     $V \leftarrow [V_{1:l}, \mathbf{v}_t]$ 
12:     $\mathbf{k}_t[0] \leftarrow 0$ 
13:     $\mathbf{q}_t[0] \leftarrow 0$ 
14:  return  $K, V, \mathbf{q}_t, \mathbf{k}_t$ 
    
```

Based on α_t , a decision is made whether KV representations \mathbf{k}_t and \mathbf{v}_t are **appended** to the cache or **accumulated** with its last element (Figure 1). In particular, for accumulation we perform a weighted average based on a predicted importance scores ω for the current token and the running sum of importance scores z_t for all the tokens since the last time step $\alpha = 0$ was predicted.

In fact, the α variable effectively segments the input sequence: each decision determines if the current segment should continue ($\alpha = 1$) or a new segment should be opened ($\alpha = 0$). As a result, after the update, the cache length for DMC is $l = \sum_{i=1}^t (1 - \alpha_i) \leq t$, whereas in vanilla Transformers it is always $l = t$. In what follows, we will refer to the ratio t/l between the length t of an uncompressed cache and the compressed length l as the Compression Ratio (CR).

Finally, multi-head self-attention is calculated similarly to vanilla Transformer using KV cache sequences, with the exception that KV sequences for different heads might have different lengths. Algorithm 1 is applied to every MHSA layer and head independently.

¹Note that this choice is arbitrary as we could use any two neurons from $\{\mathbf{q}_t, \mathbf{k}_t, \mathbf{v}_t\}$.

3.2. Training

The DMC inference algorithm switches between accumulating and appending tokens to the KV cache. In order to endow LLMs with DMC, we continue pre-training them on a negligible amount of their pre-training data, gradually increasing the compression rate towards a target. However, this poses serious challenges. First, we opt for end-to-end learning via gradient descent and continuous relaxation of the decision variables. As a result, we have to define an operation for KV cache updating when $0 < \alpha < 1$, resulting in partly aggregated, partly accumulated key and value states. Second, to avoid training–inference mismatch, we must simulate the DMC behavior at inference time while parallelizing training across a sequence of tokens: as a consequence the length of K and V is *not* reduced through compression during training; rather, all intermediate states of keys and values are explicitly kept in memory and an auxiliary (gradually discretized) mask regulates query interactions. We elaborate on our solutions to these challenges below.

Gradient Estimation for Discrete Decisions The decision whether to accumulate or append at inference time is a discrete one; however, rounding $\text{sigmoid}(\mathbf{k}[0])$ to the nearest integer for training would result in a non-differentiable operation with zero gradients. Hence, we resort to stochastic reparametrization of the decision variable during training

$$\alpha_t \sim \text{Gumbel-sigmoid}(\mathbf{k}[0] - c, \tau) \in [0, 1], \quad (8)$$

where τ is the temperature² and c is a constant subtracted so that every $\alpha = 0$ at training step 0. This ensures that DMC initially performs no compression and starts the training behaving just like the vanilla Transformer.

Partial accumulations As we relax our discrete decisions, we now must define a mechanism to update the KV cache that generalizes Algorithm 1 to continuous α . Hence, we define partially accumulated states for $\alpha \in [0, 1]$ as:

$$\begin{aligned} z_0 &\leftarrow \omega_0, & z_i &\leftarrow z_{i-1}\alpha_i + \omega_i, \\ \mathbf{k}_0 &\leftarrow \mathbf{k}_0, & \mathbf{k}_i &\leftarrow \frac{\alpha_i \mathbf{k}_{i-1} z_{i-1} + \mathbf{k}_i \omega_i}{z_i}, \\ \mathbf{v}_0 &\leftarrow \mathbf{v}_0, & \mathbf{v}_i &\leftarrow \frac{\alpha_i \mathbf{v}_{i-1} z_{i-1} + \mathbf{v}_i \omega_i}{z_i}. \end{aligned} \quad (9)$$

Note that when $\alpha \in \{0, 1\}$, Equation (9) defaults to Algorithm 1.

Intermediate compression steps Aside from key and value computations shown in Equation (9), the rest of the forward pass can be performed in parallel for all tokens in

²Low temperatures sharpen α_t into almost-discrete values which accurately mimics inference behavior.

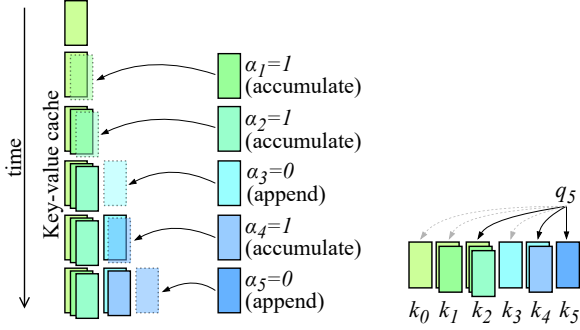


Figure 2: An example of KV cache growth in DMC during inference (left). During training (right), we retain all intermediate states seen during inference and gradually block access to some of them (gray arrows)

the sequence. Nonetheless, this creates a mismatch between training and evaluation, since all intermediate states of keys and values are accessible during self-attention.

To illustrate this issue, consider the example of a KV cache during DMC inference shown in Figure 2 for the sequence of decision scores $\alpha_{1:5} = (1, 1, 0, 1, 0)$ (importance scores ω have been omitted for clarity). The last element of the KV cache changes at every time step. In order to properly simulate the inference-time evolution of the KV cache during training, we keep all unrolled intermediate KV cache items. In lieu of an auto-regressive ‘causal’ mask, however, we use an additive mask based on the sequence of α values to modify the attention scores a_{ij}^h from Equation (4), which is shown in Figure 3. During training, the α values 1) naturally converge towards 0 or 1 as the model strives to satisfy the language modeling criterion and reduce uncertainty; 2) are intentionally pushed to almost-discrete states by the Gumbel noise and low temperature setting. Such binarization of α values significantly impacts the attention scores - it strengthens the queries interactions with last elements of every key-value segment, and weakens those with the intermediate elements, which are discarded during inference.³ In fact, when $\alpha \in \{0, 1\}$, the matrix is filled with either 0 or $-\infty$ values, and exactly corresponds to the inference time query-to-key attendance pattern.

Training objective The model is incentivized to compress the KV cache to a certain CR, and thus increase the predicted α values. Instead of matching the desired rate for each append-or-accumulate decision α , we calculate a *global* one-sided loss as the difference between the expected sum of KV tokens across all layers l , heads h and time steps t under the desired Compression Rate CR and the sum of all decisions, normalized by $(n_l n_h n)$:

³See Appendix F for details on the mask implementation.

$$\begin{array}{c}
 \mathbf{q}_0 \\
 \mathbf{q}_1 \\
 \mathbf{q}_2 \\
 \vdots \\
 \mathbf{q}_n
 \end{array}
 \begin{bmatrix}
 \mathbf{k}_0 & \mathbf{k}_1 & \mathbf{k}_2 & \dots & \mathbf{k}_n \\
 0 & -\infty & -\infty & \dots & -\infty \\
 \log(1 - \alpha_1) & 0 & -\infty & \dots & -\infty \\
 \log(1 - \alpha_1) & \log(1 - \alpha_2) & 0 & \dots & -\infty \\
 \vdots & \vdots & \vdots & \ddots & \vdots \\
 \log(1 - \alpha_1) & \log(1 - \alpha_2) & \log(1 - \alpha_3) & \dots & 0
 \end{bmatrix}$$

Figure 3: Additive mask applied during training to the the normalized attention scores to block queries from attending intermediate KV states (as well as future states).

$$\ell_{\text{CR}} = \frac{1}{n_l n_h n} * \max\left(0, \frac{n_l n_h n}{\text{CR}} - \sum_{l=1}^{n_l} \sum_{h=1}^{n_h} \sum_{t=1}^n \alpha_{lht}\right). \quad (10)$$

It is added to the language modeling loss term $\ell_{\text{LM}} = -\sum_{t=1}^n \log p_{\theta}(\mathbf{x}_t | \mathbf{x}_{<t})$, with the final objective of the training being:

$$\arg \min_{\theta} \ell_{\text{LM}} + \ell_{\text{CR}}. \quad (11)$$

Importantly, the training procedure is designed for slowly ramping up the desired compression rate and stopping at will. This enables producing a series of models with different compression rates within a single run. It follows that all hyperparameters, like Gumbel-sigmoid sampling temperature and learning rate, are not decayed and remain constant throughout training.

3.3. Practical Considerations

Implementing a variable-length cache without padding DMC allows every head to learn a custom compression, which results in KV cache sequences with variable lengths across heads. One could implement this cache naïvely with padded tensors. Foreshadowing our results in Section 5.2, however, the largest efficiency gains during inference stem from the reduced memory footprint, which allows us to increase the batch size and dramatically improve throughput. In order to get these benefits, the memory cannot be wasted on storing KV cache as padded tensors.

Thus, we provide a simple custom implementation of attention in PyTorch, building on FlashAttention (Dao et al., 2022) and PagedAttention (Kwon et al., 2023), in which the heads can learn wildly different compression rates but which does not require padding. As an ablation, we also study a constrained variant (DMC-C) in which we force the heads in a given layer to maintain similar compression rates, which minimizes the padding necessary in naïve attention implementations; however, it significantly constrains

the learned compression schema and leads to worse model quality.

Window grouping approximation The calculation of partial accumulations, during training of DMC models Equation (9), for a sequence of n tokens requires $O(n)$ sequential steps, therefore considerably slowing down the training. In order to improve the time complexity, we calculate Equation (9) at every time step t independently over a short window of the last w elements up to time t (e.g., $w = 12$). This enables us to reduce the span of computation to $O(w)$, provided that at least n threads can execute the computation in parallel for each of the n positions.

4. Experimental Setup

Baselines In our experiments, we evaluate strategies to retrofit a state-of-the-art Large Language Model (LLM), Llama 2 (Touvron et al., 2023),⁴ into a more efficient model across various sizes: 7B, 13B, and 70B. In addition to comparing the downstream performance of DMC with the original model, we also use Grouped Query Attention (GQA) as a main baseline, as it constitutes the most widespread strategy to ensure KV cache efficiency (Jiang et al., 2023).

Checkpoint adaptation To equip the original Llama 2 with GQA, we perform the standard checkpoint conversion proposed by Ainslie et al. (2023): the key and value projection matrices are split by head. Then the resulting sub-matrices corresponding to heads in the same group are merged. Note that this results in a fixed CR during training.

As for DMC, we avoid the introduction of new parameters by re-purposing the first dimension from both the \mathbf{k}_t and \mathbf{q}_t representations, in order to predict segmentation decisions and importance scores. Setting \mathbf{q}_t and \mathbf{k}_t to zero triggers a significant increase in language modeling loss, by disrupting the attention scores. To counteract this spike in loss, we pre-train the model to disregard the first dimension of \mathbf{k}_t and \mathbf{q}_t in the attention calculations. Specifically, we load the raw pre-trained weights and up-train the model for 1 billion tokens (250 steps), annealing the values of \mathbf{k}_t and \mathbf{q}_t to 0 according to the following formula:

$$\begin{aligned} \mathbf{q}_t[0] &\leftarrow \mathbf{q}_t[0] \times (1 - (t/n_t)) \\ \mathbf{k}_t[0] &\leftarrow \mathbf{k}_t[0] \times (1 - (t/n_t)) \end{aligned} \quad (12)$$

where t is the current step and $n_t = 250$. After this initial phase, which allows the model to ignore the first dimension of keys and values for attention calculations, we start the main retrofitting phase. We set the constant from Equation (8) as $c = -5$ in order to perform no compression at the start.

⁴Obtained from <https://huggingface.co/meta-llama>.

Training hyperparameters We follow the training hyperparameters outlined by Touvron et al. (2023). We employ the AdamW optimizer with parameters $\beta_1 = 0.9$, $\beta_2 = 0.95$, and $\epsilon = 1e - 5$, in conjunction with a weight decay of 0.1 and gradient clipping of 1.0. The batch size is 1024 with a context length of 4096. We apply a constant learning rate identical to the final rate from the original Llama 2 pre-training phase: 3×10^{-4} for the 7B and 13B models, and 1.5×10^{-4} for the 70B model. Finally, we set the window size (Section 3.3) to 12, and keep the Gumbel-sigmoid temperature constant at 0.1 throughout the entire training.

Training schedule The volume of data for continued pre-training of DMC is contingent on the targeted KV cache compression ratio; a larger CR necessitates more data. We use a training schedule with 24B, 48B, and 72B tokens for training to 2 \times , 3 \times , and 4 \times compression, respectively. In Appendix D we include an ablation where we use a schedule with twice less data.

For DMC, we discovered that the annealing strategy was crucial. Starting the training without compression and its measured increase helps to preserve the original perplexity. Through extensive ablations (see Appendix D), we found that any significant increase of perplexity, even if recovered during continued pre-training, prevents the model from regaining its performance on downstream tasks. The target CR is linearly increased from 1 \times to 4 \times for the 7B and 13B models, and from 1 \times to 2 \times for the 70B model.⁵

Upon achieving the target compression ratio with the DMC model, we initiate a final solidifying phase wherein we: 1) continue up-training for an additional 8B tokens, 2) maintain a fixed compression ratio, and 3) implement a cosine learning rate schedule, annealing it down to 10% of the initial value. This phase aims at stabilizing the model with a specific, fixed compression ratio.

Evaluation Following Touvron et al. (2023), we evaluate models on a series of downstream tasks, including MMLU (Hendrycks et al., 2021) for factuality, HumanEval (Chen et al., 2021) for Python code generation, and several question-answering datasets for common-sense reasoning: PIQA (Bisk et al., 2020), BoolQ (Clark et al., 2019), Arc-C and Arc-E (Clark et al., 2018), HellaSwag (Zellers et al., 2019), and WinoGrande (Sakaguchi et al., 2021). We report the 5-shot performance on MMLU, average pass@1 scores for HumanEval, and average 0-shot performance on common-sense benchmarks (CS-QA). For pass@1 scores we use a temperature of 0.1 and nucleus sampling (Holtzman et al., 2019) with top-p = 0.95.

⁵For Llama 2 70B, we do not up-train to 4 \times because this LLM is already pre-trained with GQA 8 \times .

Scale	Method	CR	MMLU	CS-QA	Human Eval
7B	–	–	44.6	70.5	14.0
	GQA	–	39.8	68.9	12.8
	DMC	2×	45.2	70.8	15.2
	GQA	–	34.7	68.3	14.0
13B	–	–	54.5	73.5	17.5
	GQA	–	50.2	72.7	15.9
	DMC	2×	54.8	74.2	20.7
	GQA	–	48.6	72.2	16.5
70B*	–	8×	68.8	78.0	29.6
	DMC	16×	68.8	77.9	29.9

Table 1: MMLU accuracy (Acc.), Commonsense Question Answering (CS-QA), Exact Match (EM), and Human-Eval Pass@1 for several scales (7B, 13B, and 70B) and compression rates (CRs; 1×, 2×, and 4×) of Llama 2. (*) Unlike the 7B and 13B models, the 70B model was trained with GQA which compresses the KV cache 8×. We apply additional 2× DMC compression during up-training to obtain a total compression of 16×.

5. Results

5.1. Main Results

We report the performance of the original LLM (equivalent to 1× CR) and efficient variants (DMC and GQA) in Table 1. For the original LLM we use results reproduced in our codebase as described in Appendix B.

DMC vs Original First, comparing DMC with the original LLM, we note that it even *increases* the performance in MMLU and CS-QA at 2× CR for 7B and 13B and in Human-Eval for all model scales. We speculate that this is due to the additional up-training steps, which expose LLMs to new examples. For the other combinations of downstream tasks and scales at 4× CR, DMC-R incurs negligible degradation: -0.7 in MMLU and -0.3 in CS-QA for 7B, -0.3 in MMLU and CS-QA for 13B. This encouraging finding suggests that DMC is robust across different model scales even for 4× CR. Overall, the fact that DMC is in general close or superior to the original performance makes it suitable as a drop-in replacement for KV caching to achieve higher inference efficiency.

DMC vs GQA Moreover, Table 1 allows for comparing DMC with GQA for equivalent CRs (2× and 4×). Overall, DMC *surpasses* GQA applied through up-training, in both CRs and in both scales (7B and 13B). For MMLU, the gap

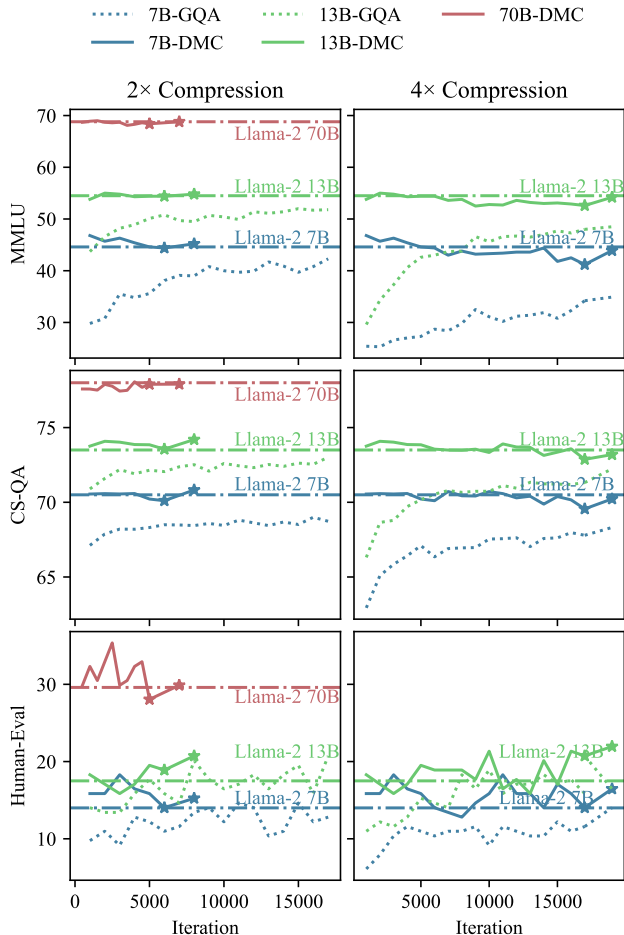
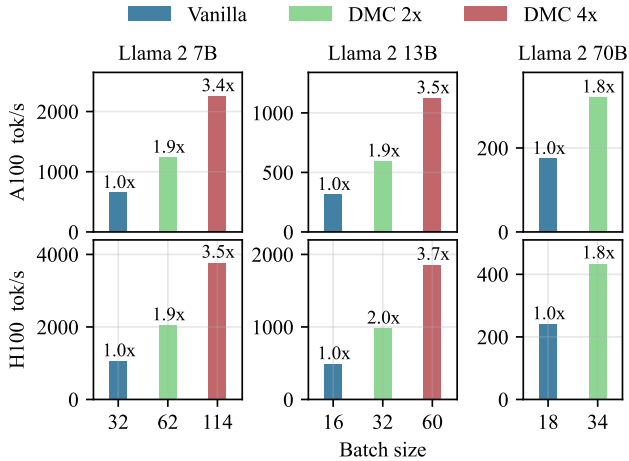


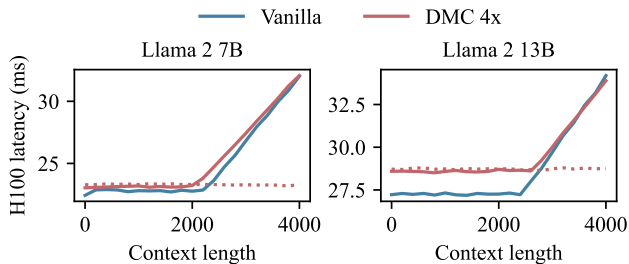
Figure 4: Sample efficiency of DMC and GQA. Horizontal lines correspond to the performance of the original Llama 2. Every DMC model was trained first with increasing CR, then with constant CR for the last 2K steps (marked with *).

widens when we increase the CR. This holds true both at the smaller 7B scale (from +5.4 for 2× CR to +9.2 for 4× CR) and at the larger 13B scale (from +4.6 for 2× CR to +5.6 for 4× CR). For CS-QA and Human-Eval, on the other hand, we observe comparable gains over GQA across CRs and model scales. These findings illustrate that DMC should be preferred to GQA for retrofitting LLMs into variants that are more efficient at inference time.

70B: DMC and GQA However, many widely adopted LLMs were pre-trained with GQA which leads to the question of whether *DMC and GQA can be used together to reap compounded benefits*. To investigate this, we retrofit Llama 2 70B, which has been pre-trained with 8× GQA. We further compress its KV cache with DMC to 2× CR: this is equivalent to a cache 16× smaller than a vanilla LLM with neither GQA nor DMC. We observe that the performance remains unchanged, and conclude that DMC and GQA can be easily and successfully combined.



(a) Inference throughput averaged over the generation of 1K tokens with 3K tokens of context (up to 4K in total). On the x-axis, we show the maximum batch size that fits in memory on a single GPU (7B and 13B) or two GPUs with tensor parallelism (70B) for the Vanilla, DMC 2x, and DMC 4x models.



(b) Latency of next token generation. Solid lines denote measurements with the maximum batch size that fits on a single GPU. Dotted lines denote DMC 4x with the same batch size as the vanilla LLM.

Figure 5: Efficiency measurements with the Megatron-LM framework on NVIDIA A100 80GB and H100 GPUs.

DMC vs DMC-C Finally, in Table 3 in Appendix E, we compare DMC with its Constrained variant DMC-C. In general, while remaining superior to GQA, DMC-C displays a significant degradation in several configurations, most notably 7B 4x where it records a drop of -6.4 in MMLU compared to the ceiling. On the other hand, DMC recovers all performance loss in DMC-C. When used in combination with custom attention implementations which does not require excessive padding, standard DMC should therefore be vastly preferred, as it retains the original LLM performance while reaping the advantages in memory efficiency fully.

Sample Efficiency To shed light on the sample efficiency of DMC and GQA, we report their performance on MMLU, CS-QA, and Codex-Eval across retrofitting steps in Figure 4. First, for a target CR of 2x, it emerges how GQA cannot achieve the performance that DMC obtains after fine-tuning

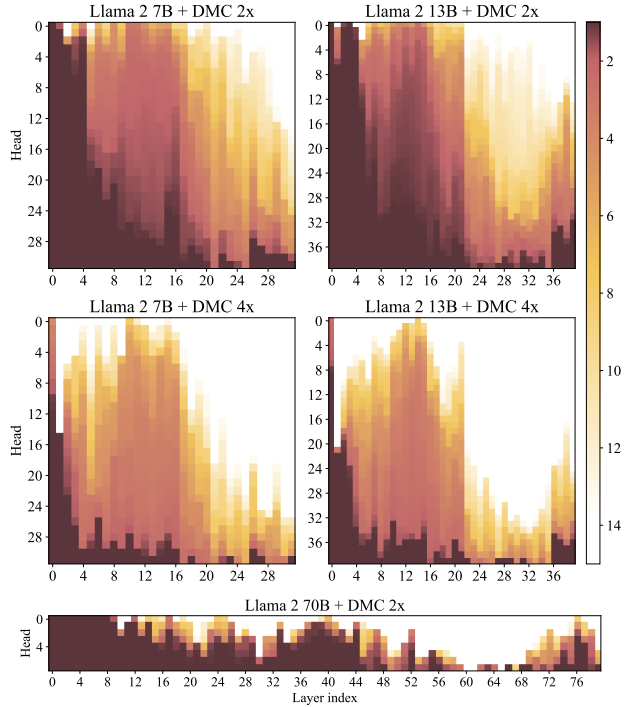


Figure 6: Heatmaps of average compression rates across layers (X-axis) and heads (Y-axis). Heads are arranged from the highest compression to the lowest top-down for clarity.

(at 8K steps) even after more than double the amount of fine-tuning (at 17K steps). This applies to both 7B and 13B scales. Figure 4 also reveals the importance of the fine-tuning phase in DMC: a limited amount of extra steps with a fixed CR recovers a significant amount of the original performance (especially for higher target CRs such as 4x).

5.2. Throughput and Latency Measurements

To verify whether increased CRs result in concrete efficiency gains, in Figure 5 we present the performance properties of DMC, estimated within the NVIDIA Megatron-LM framework (Narayanan et al., 2021). Specifically, we run measurements on a single GPU (NVIDIA A100 80GB SXM or H100 SXM) in bfloat16 precision for Llama 7B and 13B. For Llama 70B, we run the same measurements on two GPUs of the same type with tensor parallelism. We feed the model with 2K tokens of English text, and generate additional 2K tokens in an auto-regressive manner to ensure that the model properly compresses its own generations. The reported throughput consists of the average over the last 1K tokens. We limit the sequence to 4K tokens to avoid issues with context length extrapolation, as this is the maximum length observed by Llama 2 during pre-training.

In order to maximize the utilization of the GPU, we increase the batch size to the maximum that fits into memory (see

Appendix A for details). The compression of the KV cache with DMC allows for substantial increases in batch size and thus significant throughput gains. As shown in Figure 5a, DMC 2 \times translates into an effective increase in tokens per second compared to the original LLM of $> 1.8\times$ for 7B, 13B, and 70B on both A100 and H100 GPUs. Similarly, DMC 4 \times translates between 3.4 \times and 3.7 \times . This means that the efficiency boost observed in practice is very close to the theoretical limit. In addition, the extra memory saved with DMC could also be used to cache longer contexts.

Finally, we compare the latency of the original LLM with DMC 4 \times in Figure 5b. When we fit the largest possible batch size for either model, after generating approximately 2200 tokens, the inference time begins to scale linearly with the context size due to the increasingly dominating cost of reading the KV cache from the high bandwidth memory (HBM). On the other hand, if we choose to maintain the same batch size as for the original LLM also for DMC 4 \times , the memory footprint of the KV cache is reduced and latency for longer contexts improves significantly.

While we acknowledge that the behavior of LLMs at inference time depends on a multitude of factors and implementation details, our measurements in Figure 5 offer evidence that DMC increases throughput and reduces the latency of autoregressive generation with LLMs. We speculate that in the future, DMC might be used to grow the KV cache sub-linearly, which would provide an alternative between vanilla Transformers and State Space Models, where memory is constant (Fu et al., 2023; Gu & Dao, 2023).

5.3. Per-Head Learned Compression Rates

Since the training loss does not enforce any compression schema *a priori*, as it just requires to match a certain *global* CR, we can investigate what schema the model discovers in practice. In Figure 6, we report the CR for each layer and head for different scales (7B, 13B, and 70B) and CRs (2 \times and 4 \times). From all schema, it emerges how compressing deeper layers (> 16 for 7B, > 22 for 13B, > 44 for 70B) is universally the most popular strategy. However, the very final layers are compressed to a somewhat reduced degree. Fascinatingly, 4 \times DMC achieves extremely high CRs for several heads also in the few layers after the very first one. This is counter-productive as token representations are not contextualized yet, which makes taking the correct decision (whether to append or accumulate) hard.

This same pattern (in terms of relative preference for compressing the certain ranges of layers) also corresponds to how the distribution of CRs across layers changes throughout training steps, as we keep annealing the auxiliary loss ℓ_{CR} towards the target CR. Figure 7 in Appendix C illustrates how CR increases first in deeper layers, then in some non-contiguous intermediate ranges.

6. Related Work

Efficient inference in Transformer models is a subject of extensive research, with detailed overviews provided by several surveys (Pope et al., 2022; Treviso et al., 2022). This section narrows its focus to advancements in Transformer inference efficiency through KV cache size reduction.

Grouped Query Attention (GQA; Ainslie et al., 2023) represents the most widespread strategy, evolving from Multi Query Attention (MQA; Shazeer, 2019). GQA reduces the number of KV heads by allocating shared KV representations across subsets of query heads. Prior efforts in token merging (Zhang et al., 2018) condensed the entire past context into a single token, while (Liu et al., 2018; Rae et al., 2019) employed strided convolution and mean pooling kernels to reduce the number of KV tokens. Sliding window attention techniques (Beltagy et al., 2020; Child et al., 2019) restrict attention to a maximum of w preceding tokens. Though effective in limiting KV cache, such methods perform *fixed-size* compression, unlike the presented *dynamic* DMC, which adapts the compression schema based on the input sequence. This yields superior results, as we prove in an ablation in Appendix E.

Previous learnable compression methods (Anagnostidis et al., 2023, *inter alia*) decide which tokens to drop from the KV cache. DMC takes a different approach as instead of dropping tokens it merges them. Hence, it preserves cached information more faithfully. Moreover, the DMC compression mechanism has constant complexity with respect to the context length, while the one proposed by Anagnostidis et al. (2023) is linear. Mu et al. (2023) instead compresses prompts through costly generation which limits their inference benefits. Moreover, this method is only applicable to compressing the model input while DMC compresses *on-the-fly* the entire sequence, including both the model input and the generated output.

Non-learnable cache eviction strategies (Zhang et al., 2023; Sheng et al., 2023; Liu et al., 2023; Wang et al., 2020; Ge et al., 2023) utilize attention scores or token properties to filter tokens in the KV cache. These approaches, while bypassing additional training, rely on heuristics and lack the ability to learn the compression mechanisms. In contrast, DMC integrates compression into its learning objective in an end-to-end manner, where compression is synergistic to language generation.

Finally, DMC draws inspiration from Dynamic Token Pooling (Nawrot et al., 2022), which introduces a learnable boundary predictor to merge the representations of groups of tokens in intermediate layers. DMC improves upon this idea by applying it to the KV cache of and introducing a continuous relaxation of the pooling decision during training. Moreover, it enables retrofitting pre-trained LLMs with

minimal extra steps rather than training language models from scratch.

7. Conclusions and Future Work

We proposed Dynamic Memory Compression, a method to reduce the length of the KV cache in Transformers, which enhances the memory efficiency and speed of LLMs at inference time. For every new token, DMC learns end-to-end whether to append its KV representations to the cache or merge them with the top element in the cache. We show how to retrofit LLMs such as Llama 2 at different scales (7B, 13B, and 70B) into efficient DMC versions with a negligible amount of extra data and without extra parameters. DMC LLMs with $2\times$ and $4\times$ compression rates (CRs) retain (or even improve upon) the performance of the original LLM. In addition, we demonstrate that, for comparable CRs, DMC has significantly higher continued pre-training performance and sample efficiency than Grouped Query Attention (GQA), a widespread method for KV cache size reduction.

Impact Statement

Dynamic Memory Compression in Large Language Models (LLMs) like Llama 2 results in better computational efficiency, reducing both operational costs and environmental impact (Patterson et al., 2021). By enabling higher throughput and lower latency, DMC democratizes access to advanced AI, making state-of-the-art models suitable for a broader range of hardware. This may not only accelerate innovation across diverse sectors but also promote AI development and applications in an environmentally conscious manner.

References

- Ainslie, J., Lee-Thorp, J., de Jong, M., Zemlyanskiy, Y., Lebrón, F., and Sanghai, S. K. GQA: Training generalized multi-query transformer models from multi-head checkpoints. *ArXiv*, abs/2305.13245, 2023.
- Anagnostidis, S., Pavllo, D., Biggio, L., Noci, L., Lucchi, A., and Hofmann, T. Dynamic context pruning for efficient and interpretable autoregressive transformers. *ArXiv*, abs/2305.15805, 2023.
- Bahdanau, D., Cho, K., and Bengio, Y. Neural machine translation by jointly learning to align and translate. *ArXiv*, abs/1409.0473, 2014.
- Beltagy, I., Peters, M. E., and Cohan, A. Longformer: The long-document transformer. *ArXiv*, abs/2004.05150, 2020.
- Bisk, Y., Zellers, R., Le bras, R., Gao, J., and Choi, Y. PIQA: Reasoning about physical commonsense in natural language. *Proceedings of the AAAI Conference on Artificial Intelligence*, 34(05), Apr. 2020.
- Bolya, D., Fu, C.-Y., Dai, X., Zhang, P., Feichtenhofer, C., and Hoffman, J. Token merging: Your ViT but faster. *ArXiv*, abs/2210.09461, 2022.
- Chen, M., Tworek, J., Jun, H., Yuan, Q., Ponde, H., Kaplan, J., Edwards, H., Burda, Y., Joseph, N., Brockman, G., Ray, A., Puri, R., Krueger, G., Petrov, M., Khlaaf, H., Sastry, G., Mishkin, P., Chan, B., Gray, S., Ryder, N., Pavlov, M., Power, A., Kaiser, L., Bavarian, M., Winter, C., Tillet, P., Such, F. P., Cummings, D. W., Plappert, M., Chantzis, F., Barnes, E., Herbert-Voss, A., Guss, W. H., Nichol, A., Babuschkin, I., Balaji, S., Jain, S., Carr, A., Leike, J., Achiam, J., Misra, V., Morikawa, E., Radford, A., Knight, M. M., Brundage, M., Murati, M., Mayer, K., Welinder, P., McGrew, B., Amodei, D., McCandlish, S., Sutskever, I., and Zaremba, W. Evaluating large language models trained on code. *ArXiv*, abs/2107.03374, 2021.
- Child, R., Gray, S., Radford, A., and Sutskever, I. Generating long sequences with sparse transformers. *ArXiv*, abs/1904.10509, 2019.
- Choromanski, K., Likhoshesterov, V., Dohan, D., Song, X., Gane, A., Sarlós, T., Hawkins, P., Davis, J., Mohiuddin, A., Kaiser, L., Belanger, D., Colwell, L. J., and Weller, A. Rethinking attention with Performers. *ArXiv*, abs/2009.14794, 2020.
- Clark, C., Lee, K., Chang, M.-W., Kwiatkowski, T., Collins, M., and Toutanova, K. BoolQ: Exploring the surprising difficulty of natural yes/no questions. In Burstein, J., Doran, C., and Solorio, T. (eds.), *Proceedings of the 2019 Conference of the North American Chapter of the Association for Computational Linguistics*, Minneapolis, Minnesota, June 2019. Association for Computational Linguistics.
- Clark, P., Cowhey, I., Etzioni, O., Khot, T., Sabharwal, A., Schoenick, C., and Tafjord, O. Think you have solved question answering? try ARC, the AI2 reasoning challenge. *ArXiv*, abs/1803.05457, 2018.
- Dao, T., Fu, D., Ermon, S., Rudra, A., and Ré, C. FlashAttention: Fast and memory-efficient exact attention with IO-awareness. In Koyejo, S., Mohamed, S., Agarwal, A., Belgrave, D., Cho, K., and Oh, A. (eds.), *Advances in Neural Information Processing Systems*, volume 35. Curran Associates, Inc., 2022.
- Fu, D. Y., Dao, T., Saab, K. K., Thomas, A. W., Rudra, A., and Re, C. Hungry hungry hippos: Towards language modeling with state space models. In *The Eleventh International Conference on Learning Representations*, 2023.

- Ge, S., Zhang, Y., Liu, L., Zhang, M., Han, J., and Gao, J. Model tells you what to discard: Adaptive kv cache compression for llms. *ArXiv*, abs/2310.01801, 2023.
- Gu, A. and Dao, T. Mamba: Linear-time sequence modeling with selective state spaces. *ArXiv*, abs/2312.00752, 2023.
- Hendrycks, D., Burns, C., Basart, S., Zou, A., Mazeika, M., Song, D., and Steinhardt, J. Measuring massive multitask language understanding. In *International Conference on Learning Representations*, 2021.
- Holtzman, A., Buys, J., Du, L., Forbes, M., and Choi, Y. The curious case of neural text degeneration. *ArXiv*, abs/1904.09751, 2019.
- Jiang, A. Q., Sablayrolles, A., Mensch, A., Bamford, C., Chaplot, D. S., de las Casas, D., Bressand, F., Lengyel, G., Lample, G., Saulnier, L., Lavaud, L. R., Lachaux, M.-A., Stock, P., Scao, T. L., Lavril, T., Wang, T., Lacroix, T., and Sayed, W. E. Mistral 7B. *ArXiv*, abs/2310.06825, 2023.
- Kim, G. and Cho, K. Length-adaptive Transformer: Train once with length drop, use anytime with search. In *Annual Meeting of the Association for Computational Linguistics*, 2020.
- Kwon, W., Li, Z., Zhuang, S., Sheng, Y., Zheng, L., Yu, C. H., Gonzalez, J. E., Zhang, H., and Stoica, I. Efficient memory management for large language model serving with pagedattention. *Proceedings of the 29th Symposium on Operating Systems Principles*, 2023.
- Liu, P. J., Saleh, M., Pot, E., Goodrich, B., Sepassi, R., Kaiser, L., and Shazeer, N. M. Generating wikipedia by summarizing long sequences. *ArXiv*, abs/1801.10198, 2018.
- Liu, Z., Desai, A., Liao, F., Wang, W., Xie, V., Xu, Z., Kyrillidis, A., and Shrivastava, A. Scissorhands: Exploiting the persistence of importance hypothesis for llm kv cache compression at test time. *ArXiv*, abs/2305.17118, 2023.
- Mu, J., Li, X. L., and Goodman, N. D. Learning to compress prompts with gist tokens. *ArXiv*, abs/2304.08467, 2023.
- Narayanan, D., Shoeybi, M., Casper, J., LeGresley, P., Patwary, M., Korthikanti, V. A., Vainbrand, D., Kashinkunti, P., Bernauer, J., Catanzaro, B., Phanishayee, A., and Zaharia, M. A. Efficient large-scale language model training on gpu clusters using megatron-lm. *SC21: International Conference for High Performance Computing, Networking, Storage and Analysis*, 2021.
- Nawrot, P., Chorowski, J., Lańcucki, A., and Ponti, E. Efficient transformers with dynamic token pooling. In *Annual Meeting of the Association for Computational Linguistics*, 2022.
- Patterson, D. A., Gonzalez, J., Le, Q. V., Liang, C., Munguía, L.-M., Rothchild, D., So, D. R., Texier, M., and Dean, J. Carbon emissions and large neural network training. *ArXiv*, abs/2104.10350, 2021.
- Pope, R., Douglas, S., Chowdhery, A., Devlin, J., Bradbury, J., Levenskaya, A., Heek, J., Xiao, K., Agrawal, S., and Dean, J. Efficiently scaling transformer inference. *ArXiv*, abs/2211.05102, 2022.
- Rae, J. W., Potapenko, A., Jayakumar, S. M., and Lillicrap, T. P. Compressive transformers for long-range sequence modelling. *ArXiv*, abs/1911.05507, 2019.
- Sakaguchi, K., Bras, R. L., Bhagavatula, C., and Choi, Y. WinoGrande: An adversarial winograd schema challenge at scale. *Commun. ACM*, 64(9), 2021.
- Shazeer, N. M. Fast transformer decoding: One write-head is all you need. *ArXiv*, abs/1911.02150, 2019.
- Sheng, Y., Zheng, L., Yuan, B., Li, Z., Ryabinin, M., Fu, D. Y., Xie, Z., Chen, B., Barrett, C. W., Gonzalez, J., Liang, P., Ré, C., Stoica, I., and Zhang, C. High-throughput generative inference of large language models with a single gpu. In *International Conference on Machine Learning*, 2023.
- Touvron, H., Martin, L., Stone, K., Albert, P., Almahairi, A., Babaei, Y., Bashlykov, N., Batra, S., Bhargava, P., Bhosale, S., Bikel, D., Blecher, L., Ferrer, C. C., Chen, M., Cucurull, G., Esiobu, D., Fernandes, J., Fu, J., Fu, W., Fuller, B., Gao, C., Goswami, V., Goyal, N., Hartshorn, A., Hosseini, S., Hou, R., Inan, H., Kardas, M., Kerkez, V., Khabsa, M., Kloumann, I., Korenev, A., Koura, P. S., Lachaux, M.-A., Lavril, T., Lee, J., Liskovich, D., Lu, Y., Mao, Y., Martinet, X., Mihaylov, T., Mishra, P., Molybog, I., Nie, Y., Poulton, A., Reizenstein, J., Rungta, R., Saladi, K., Schelten, A., Silva, R., Smith, E. M., Subramanian, R., Tan, X. E., Tang, B., Taylor, R., Williams, A., Kuan, J. X., Xu, P., Yan, Z., Zarov, I., Zhang, Y., Fan, A., Kambadur, M., Narang, S., Rodriguez, A., Stojnic, R., Edunov, S., and Scialom, T. Llama 2: Open foundation and fine-tuned chat models. *ArXiv*, abs/2307.09288, 2023.
- Treviso, M. V., Ji, T., Lee, J.-U., van Aken, B., Cao, Q., Ciosici, M. R., Hassid, M., Heafield, K., Hooker, S., Martins, P. H., Martins, A. F. T., Milder, P., Raffel, C., Simpson, E., Slonim, N., Balasubramanian, N., Derczynski, L., and Schwartz, R. Efficient methods for natural language processing: A survey. *Transactions of the Association for Computational Linguistics*, 11, 2022.
- Vaswani, A., Shazeer, N. M., Parmar, N., Uszkoreit, J., Jones, L., Gomez, A. N., Kaiser, L., and Polosukhin, I. Attention is all you need. In *Neural Information Processing Systems*, 2017.

Wang, H., Zhang, Z., and Han, S. Spatten: Efficient sparse attention architecture with cascade token and head pruning. *2021 IEEE International Symposium on High-Performance Computer Architecture (HPCA)*, 2020.

Zellers, R., Holtzman, A., Bisk, Y., Farhadi, A., and Choi, Y. HellaSwag: Can a machine really finish your sentence? In Korhonen, A., Traum, D., and Màrquez, L. (eds.), *Proceedings of the 57th Annual Meeting of the Association for Computational Linguistics*, Florence, Italy, July 2019. Association for Computational Linguistics.

Zhang, B., Xiong, D., and Su, J. Accelerating neural transformer via an average attention network. *ArXiv*, abs/1805.00631, 2018.

Zhang, Z. A., Sheng, Y., Zhou, T., Chen, T., Zheng, L., Cai, R., Song, Z., Tian, Y., Ré, C., Barrett, C. W., Wang, Z., and Chen, B. H2o: Heavy-hitter oracle for efficient generative inference of large language models. *ArXiv*, abs/2306.14048, 2023.

Appendix

A. Memory-Bound Operations in Transformers

During autoregressive generation with a KV cache, the sequence length during every forward pass is $n = 1$. The vast majority of time is spent on calculations for linear layers and multi-head self-attention. For linear layers, the ratio of FLOPs to input bytes improves as the batch size increases. For small batch sizes, the operations are memory bounded on reading the weight matrices from HBM. On the other hand, for MHSA layers during inference the ratio of FLOPs to input bytes does not change and MHSA layers are always memory bounded on current GPUs. The impact of KV cache compression is two-fold as it 1) allows us to decrease the latency of MHSA layers, and 2) allows us to fit larger batch sizes in HBM, resulting in better throughput and better utilization of GPUs during the calculations of linear layers.

B. Replicating the Original Results

To make sure that our implementation is correct, for each downstream task we compare the performance reported in the original Llama 2 paper (Touvron et al., 2023) with those obtained from the Hugging Face Hub checkpoints. Furthermore, we evaluate the impact of using our internal data mixture for up-training, acknowledging that variations in data proportions and preprocessing methodologies can influence model behavior. In particular, we up-train the vanilla pre-trained Llama-2 checkpoint for 200 training steps, amounting to 1B tokens, in accordance with the original Llama-2 training schedule. We compute the average and standard deviation of checkpoints after 50, 100, 150, 200 steps. In our experiments, we replicate the results reported by the Llama 2 paper almost exactly, as shown in Table 2.

C. Analysis of the Compression Schema Learned by DMC

Evolution Throughout the Training In Figure 7, we illustrate how the CR changes for each layer of the Llama 2 7B model throughout the training from $1\times$ up to $4\times$ global CR. Each subplot corresponds to a different global CR which occurs at different stages of the training, going from the smallest (1.17) at the top, to the highest (4.16) at the bottom. There is a clear trend such that, for a smaller global Compression Ratio (i.e. at the beginning of the training), the model emphasizes compression in the later layers. As the global Compression Ratio increases, the model keeps on compressing in final layers but also starts to compress the earlier layers. We hypothesize that the token representations in the initial layers do not contain sufficient information to perform any meaningful grouping. Conversely, token

representations in the subsequent layers are more defined and, possibly, after several attention layers, already contain redundant/shared information.

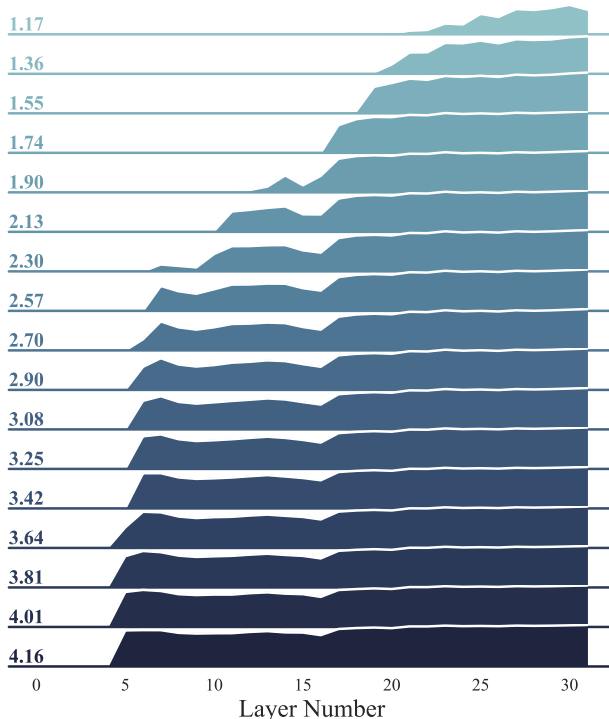


Figure 7: Compression distribution across layers at different stages of retrofitting a Llama 2 7B model. We adhere to the convention where, for a given subplot, a larger space above a given layer indicates greater compression at that layer.

Sequence Length versus Compression Ratio Do DMC models compress sequences with a uniform CR independent from their total length? We find that this is not the case. As show by Figure 8, the CR increases logarithmically as we increase the total sequence length. This holds true across all global CRs (including both $2\times$ and $4\times$).

Absolute Position versus Compression Decision Do DMC models learn a fixed compression schema, or do they exhibit position biases? In Figure 9, we plot the average value of the decision variable α across positions in the sequence (0 to 4096). Our observations reveal that the average value of the decision variable α is independent of a token’s position in the input sequence which demonstrates that the model does not follow some fixed pattern. This persists across both $2\times$ and $4\times$ compression ratios (CR).

Compression Schemata learned by DMC-C Studying the compression schema in Figure 10 learned by DMC-C, we find a very different pattern compared to DMC, due to

	CS-QA			MMLU			Human-Eval		
	7B	13B	70B	7B	13B	70B	7B	13B	70B
Paper	70.6	73.7	78.5	45.3	54.8	68.9	12.8	18.3	29.9
Checkpoint	70.6	73.7	78.5	45.7	55.1	69.1	13.4	17.7	30.5
Up-trained	70.5 ± 0.2	73.5 ± 0.1	78.0 ± 0.1	44.6 ± 0.6	54.5 ± 0.3	68.8 ± 0.3	14.0 ± 1.2	17.5 ± 1.5	29.6 ± 1.6

Table 2: Replicating the original up-training results.

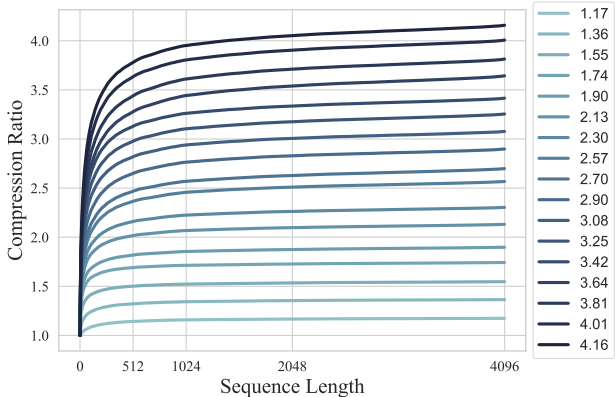


Figure 8: CR achieved by Llama 2 7B for particular sequence lengths across various global CRs.

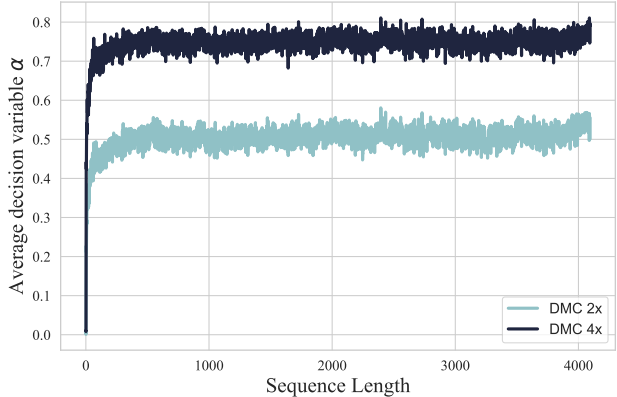


Figure 9: Average value of the decision α for positions (0, 4096) averaged over 128 samples, heads and layers.

the auxiliary loss forcing the model to compress similarly across heads in the same layer. Nevertheless, we observe a similar global preference for compressing deeper layers.

Interpretability A natural question arises, whether the compression schema that the model learns is somehow aligned with human intuitions about text segmentation. We analyzed the outputs of Llama 2 13B DMC with CR 4 and noticed that some heads compress according to the boundaries of linguistic units, such as words or syntactic phrases. Figure 11 shows the compression schema learned by head 14 in layer 0. In this case, the model merges the subwords back into words *reverting* the tokenizer. Interestingly, some groupings of tokens correspond to semantic units, e.g., “19th century”, “50 percent”, or “a week back later”. Yet, we also stress that many heads and layers are not interpretable as their behavior does not overlap with linguistic units.

More generally higher layers merge longer tokens sequences, in line with Figure 6. For instance, Figure 12 shows the decisions of layer 24 head 2. We leave a more in-depth analysis of compression schemata learned by DMC to future work.

D. Training Ablations

Training Steps per Increase in CR Another advantage of DMC is its high flexibility. In fact, based on the availability of resources, different regimes can be chosen when anneal-

ing the CR to the target during up-training. In Figure 13, we compare a SHORT and a LONG regime for the constrained variant of DMC (DMC-C), which continuously increase the CR by 1 every 3K and 6K steps (12B and 24B tokens), respectively. It is evident how there exists a trade-off between training steps (hence, time) and performance. Additionally, Figure 13 showcases another aspect of the higher flexibility DMC affords: it is compatible with arbitrary real-valued CRs, as opposed to integer CRs divisible by 2 as in GQA.

Schedules of Target CR Additionally, we explore how different schedules for the target CR impact the model performance. In the standard setup, this is annealed from 1 to the target CR throughout the duration of training. Here, we compare it with a setup where the CR used in the auxiliary loss for compression is set to the target from the start (DMC-immediate). We show the results in Figure 14. As expected, DMC-immediate has a perplexity spike at the beginning when the model quickly increases the CR due to the auxiliary loss. While perplexity is recovered during training, even to a lower point than DMC with annealing, downstream accuracy on MMLU benchmark is degraded across the board. This showcases why avoiding perplexity spikes is fundamental to successfully retrofit an LLM.

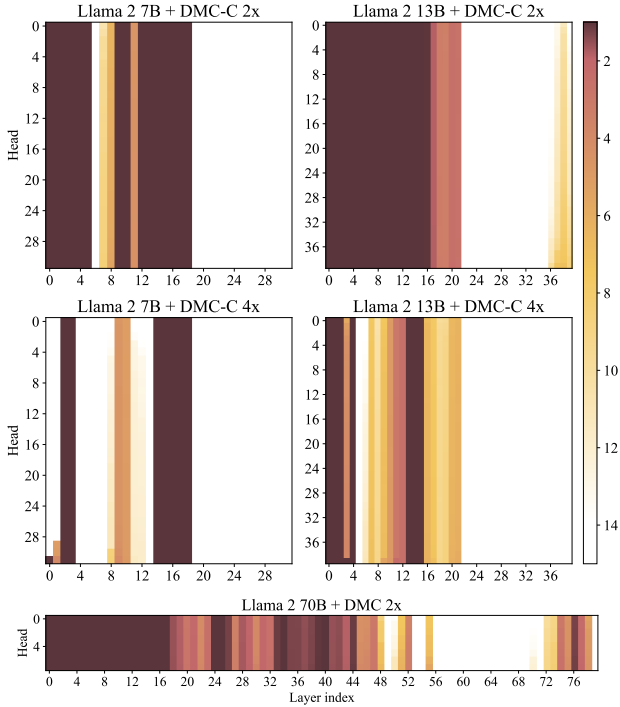


Figure 10: Heatmaps of average compression rates across layers (X-axis) and heads (Y-axis) for DMC-C. Heads are arranged from the highest compression to the lowest top-down for clarity.

E. DMC Ablations

Fixed vs Learned Memory Compression We assessed the importance of dynamically learning compression decisions in DMC by comparing it with Fixed Memory Pooling, which reduces the overall number of tokens in memory by deterministically averaging every n tokens, where n in this case is identical to the compression rate. The results, shown in Figure 14, demonstrate that the dynamic component of DMC is crucial to achieve lower perplexity as well as higher downstream accuracy.

Global vs Local (Layer-wise) Compression Prior We compare two approaches to compression: a *Local* Prior, which enforces a pre-specified compression ratio (CR) in each layer independently, requiring every layer to compress approximately the same amount, and a *Global* Prior used by default DMC, which applies a pre-specified CR across all layers, giving the model the freedom to apply different CRs in each layer, provided that their average compression equals the global CR. Figure 15 clearly indicates that the Global Prior (DMC in Figure 15) improves MMLU performance compared to the Local Prior.

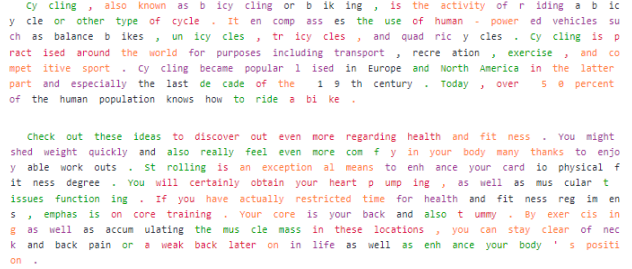


Figure 11: Compression schema found by Llama 2 13B DMC 4x in layer 0, head 14. Tokens that are merged in the KV cache are marked with the same color.

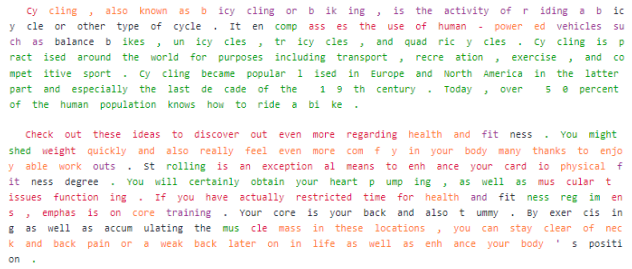


Figure 12: Compression schema found by Llama 2 13B DMC 4x for layer 24, head 2. Tokens that are merged in the KV cache are marked with the same color.

In-layer Relaxation We then compare three strategies to determine how similar compression schemata for heads within each layer should be (assuming a global prior):

1. DMC: There are no constraints on the decision and importance scores, except for the global loss nudging the model towards a pre-defined CR.
2. DMC-C: Different heads can have varying decision and importance scores within each layer. However, an auxiliary loss encourages the model to maintain similar CRs among all heads within the layer.
3. DMC-HardC: Decision scores α_t and importance scores ω_t are shared across heads, leading to the same shortening schema within each layer across heads.

As per Figure 15, the default DMC strategy shows a consistent MMLU performance across varying CRs, while both DMC-C and DMC-HardC exhibit a sharp drop in MMLU as the compression reaches 1.9x. Moreover, in Table 3 we report a more thorough comparison between DMC and DMC-C. In general, while remaining superior to GQA, DMC-C displays a significant degradation in several configurations when compared to regular DMC.

Importance Scores Finally, we assess the impact of predicting importance scores for accumulation as opposed to

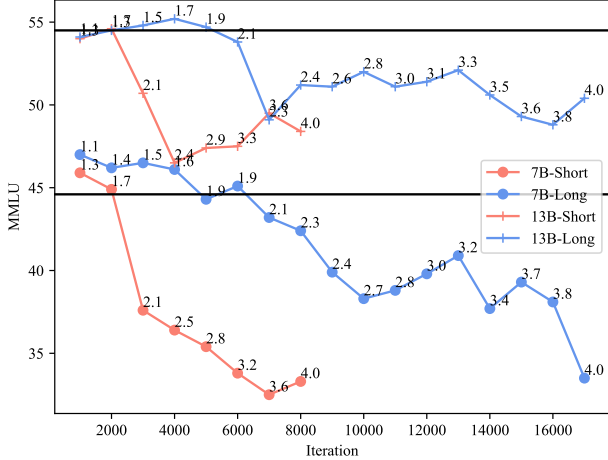


Figure 13: Different up-training regimes for DMC-C: Short (red) increases CR by 1 every 6K steps, Long (blue) increases CR by 1 every 3K steps. Horizontal lines correspond to the performance of the original Llama 2.

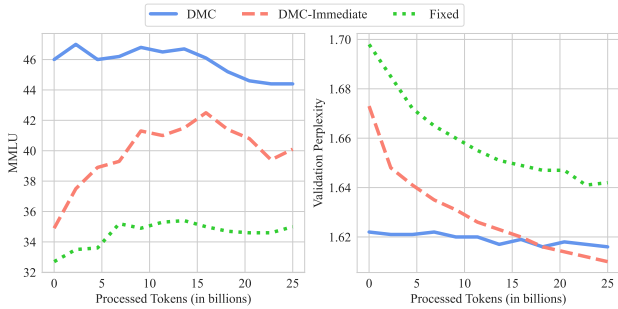


Figure 14: Validation perplexity and MMLU accuracy vs training steps for Fixed Memory Pooling and a variant of DMC where the auxiliary loss CR is immediately set to the target on the onset of training. All models follow the regular training schedule and are trained up to $2 \times$ CR.

uniformly weighting each token in a group. Figure 15 shows that DMC-C with Uniform Weighting is worse than learned weighting DMC-C.

F. Masking Implementation Details

We mask the unnormalized attention score for the pair (i, j) as follows:

$$\hat{a}_{(i,j)} = \underbrace{\frac{\mathbf{q}_i[1:d_h]^\top \mathbf{k}_j[1:d_h]}{\sqrt{d_h}}}_{\text{attention score}} + \underbrace{\log(1 - \alpha_{j+1})}_{\text{attention mask}}.$$

We rely on the memory efficient implementation of MHSA from PyTorch, which allows adding arbitrary masks to the attention scores before softmax. Notwithstanding this, at inference time DMC remains compatible with efficient libraries

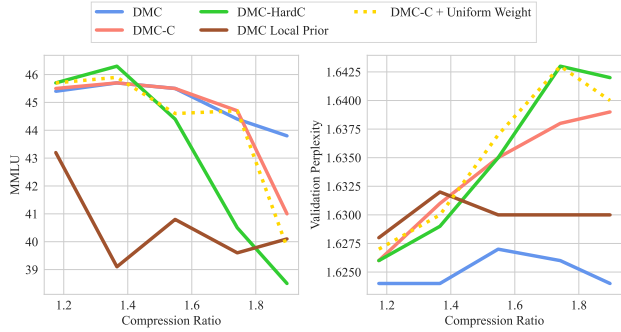


Figure 15: Validation perplexity and test MMLU accuracy vs compression rate for different types of compression priors, in-layer relaxations, and importance scores. All models follow the SHORT training regime and are trained up to $2 \times$ CR.

for attention such as Flash Attention (Dao et al., 2022). The $\log(1 - \alpha_{j+1})$ term is calculated as $\log\text{-sigmoid}(-\alpha_{j+1})$ for better numerical precision.

G. Limitations

This paper is focused on retrofitting existing LLMs into DMC variants. In our preliminary experiments with *pre-training LLMs with DMC from scratch* we obtained negative results when compared to the training curve of GQA. We speculate that this is due to the mutual dependency of modeling and segmenting data: when token representations are not of sufficient quality, boundary decisions are unreliable. Vice versa, incorrect boundary decisions may lead to poor token representations. This creates a vicious cycle which may be broken by techniques that facilitate convergence, such as an Expectation Maximization-style alternation between modeling and segmenting.

Scale	Method	CR	MMLU	CS-QA	Human Eval
7B	–	–	44.6	70.5	14.0
	GQA		39.8	68.9	12.8
	DMC	2×	45.2	70.8	15.2
	DMC-C		45.5	70.6	14.6
	GQA		34.7	68.3	14.0
	DMC	4×	43.9	70.2	16.5
	DMC-C		38.2	69.6	14.6
13B	–	–	54.5	73.5	17.5
	GQA		50.2	72.7	15.9
	DMC	2×	54.8	74.2	20.7
	DMC-C		54.8	73.9	18.3
	GQA		48.6	72.2	16.5
	DMC	4×	54.2	73.2	22.0
	DMC-C		52.4	72.9	18.3
70B*	–	8×*	68.8	78.0	29.6
	DMC	16×*	68.8	77.9	29.9
	DMC-C	16×*	67.4	78.2	31.1

Table 3: MMLU accuracy (Acc.), Commonsense Question Answering (CS-QA) Exact Match (EM), and Human-Eval Pass@1 for several scales (7B, 13B, and 70B) and compression rates (CRs; 1×, 2×, and 4×) of Llama 2. Here, we include an extra DMC variant - DMC-C, which does not require custom implementation. (*) The 70B model was trained with GQA which compresses the KV cache 8×.